

STUDYING THE TOKAMAK EQUILIBRIA USING VARIATIONAL MOMENT METHOD



A thesis submitted towards partial fulfilment of
BS-MS Dual Degree Programme

by

ADWITEEY MAURIYA

under the guidance of

DR R. SRINIVASAN AND PROF AMITA DAS

INSTITUTE FOR PLASMA RESEARCH,
GANDHINAGAR INDIA

INDIAN INSTITUTE OF SCIENCE EDUCATION AND RESEARCH
PUNE

Certificate

This is to certify that this thesis entitled "Studying The Tokamak Equilibria using Variational Moment Method" submitted towards the partial fulfilment of the BS-MS dual degree programme at the Indian Institute of Science Education and Research Pune represents original research carried out by " Adwiteey Mauriya" at "Institute for Plasma Research, Gandhinagar", under the supervision of "Dr R. Srinivasan" during the academic year 2013-2014.

Student
ADWITEEY
MAURIYA

Supervisor
DR R.SRINIVASAN

Acknowledgements

The candidate would especially like to thank Dr R. Srinivasan and Prof Amita das for their mentorship. The candidate also would like to thank to Dr Subrata Pradhan for their invaluable insightful inputs regarding the various aspects of my project. The candidate would like to thank to Mr Amit Singh to help me debugging the codes. Candidate also would like to thank to Mr Upendra to motivate me for my project. This work was undertaken under the auspices of KVPY fellowship (SX-1081134). Also, I acknowledge the Institute of Plasma Research (IPR) for the generosity regarding accomodation and the use of library. Finally, the candidate would like to thank Dr P. Subramanian for kindly agreeing to help with the coordination of this project with IISER, Pune.

Abstract

Grad Shafranov equation is equilibrium solution of ideal MHD. A variational moment method is studied to estimate the solution to the Grad-shafranov equation which is generalized to find approximate free boundary solutions to the grad-shafranov equation. Some ordinary differential equation had to be solved to calculate the poloidal magnetic flux $\psi(R, Z)$ those were nothing but Grad-Shafranov equation's moments. Grad-Shafranov equation's moment are fourier amplitudes of the inverse mapping of $R(\psi, \theta)$ and $Z(\psi, \theta)$. Numerical and Analytical solutions of moment equations are constructed whose results concur well with two dimensional equilibrium code. The main advantage of the variational moment method is that it significantly reduces the computational time required to determine two-dimensional equilibria without sacrificing accuracy. In future the code will further be developed to calculate the flux surface at separatrix and location of strike points.

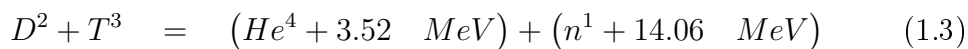
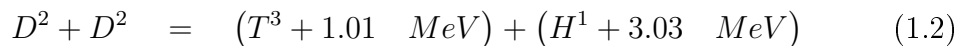
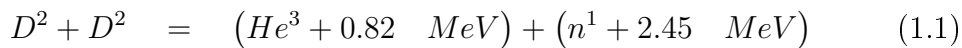
Contents

1	Introduction	3
1.1	Confinement Systems	5
1.1.1	Magnetic confinement	5
1.1.2	The tokamak concept	7
1.1.3	The tokamak	8
2	Theory	11
3	Methods	26
3.1	Introduction	26
3.2	Analytical formulation of the inverse equilibrium problem . . .	26
3.2.1	Coordinate transformation	26
3.2.2	Variational principle	27
3.3	Moments equations for the inverse mapping	32
3.3.1	Determination of fourier expansion coefficients	32
3.4	Derived quantities	37
3.4.1	Volume	37
3.4.2	Flux tube surface area	37
3.4.3	Poloidal flux	37
3.4.4	Poloidal current	37
3.4.5	Toroidal flux	38
3.4.6	Toroidal current density	38
3.4.7	Equivalent Current density	38
3.4.8	Safety factor	38
3.5	Numerical Formulation	39
4	Results	41
5	Discussion	45
	References	46

Chapter 1

Introduction

Consumption of electricity increases relentlessly and hence it is necessary to look for an alternate, safe and efficient technology to tackle the future power crisis. Nuclear fusion is one such method. In nuclear fusion, two light elements undergo an exoergic reaction to form a heavier nucleus. Fusion process is responsible for the heat production in suns and stars. The possibility of self sustained fusion reaction can form the basis for the fusion power reactor. One of the most promising reactions is the fusion of hydrogen isotopes. The reactions are :



where H, n, D, T and He indicate hydrogen, neutron, deuterium, tritium and helium respectively. The first and second reactions are equally likely, the reaction 1.3 has about 100 times combined cross-section of reactions 1.1 and 1.2 and reaction 1.4 dominates at very high impact energies above 400 keV. Energy associated with each product particle is shown in MeV. The reaction no 3 has been shown schematically in fig 1.1 Compared to fission process, fusion have several important potential advantages. First of all, the deuterium reserves are much more than that of economically recoverable fission reserve, even though the abundance of deuterium is only one part of 6700. Second the products of above reaction other than tritium are stable. Tritium is radioactive but one can not consider it as a waste. This undergoes fusion more efficiently than the deuterium and makes the power economically

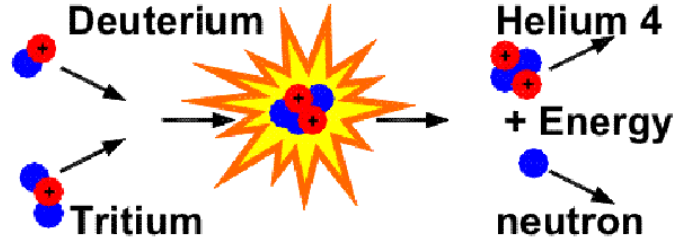


Figure 1.1: Cartoon of Nuclear reaction 1.3

viable. Third, fusion reactors would be inherently fail-safe due to the natural repulsion among the reactants and hence there will be no runaway situation.

To have a fusion reaction, two atomic nuclei have to be brought closer against their coulomb repulsion. This can be achieved by supplying heat energy to the system. The temperature of such system has to be raised around 100 million degrees. In addition to high temperature, it is necessary to have the fusion nuclei stay together for long enough to enable sufficient number of fusion reactions to occur. Confining such a hot plasma (Collection of charged particle) in the laboratory for controlled fusion is a key challenge. In the case of stars, the confinement is done by gravitational force but in the laboratory, one needs to use magnetic fields to do the same job. Fusion power from a reactor depends on the number density (n), the fusion cross-section (σv) the rate at which the fusion reaction takes place ($\propto T$), the energy confinement time (τ_E) and the plasma volume. Reactor performance is often characterized by a figure of merit $n\tau_E T$ that takes into account both the lawson criterion and the temperature dependence of reaction rate cross-section. To have a viable fusion power reactor, it is essential to maximize all of the above mentioned parameters so that the ignition condition $n\tau_E T > 3 \times 10^{24} [m^{-3}seV]$ is satisfied. Any fusion plasma confinement system must meet these requirements. Hence, it is essential to study the merits and demerits of various confinement systems and try to optimize them for a reactor.

The confinement of plasma in a toroidal geometry is one of the most advanced concepts in nuclear fusion research. In the beginning of fifties it was recognized that linear and open ended plasma devices suffer from plasma instabilities and end losses. The simplest configuration with closed field lines was discovered and found to have much better confinement properties. Re-

search and development over the last four decades have strengthened the belief that tokamak is a leading plasma confinement concept. A brief description of toroidal confinement concept is given in the next section.

1.1 Confinement Systems

1.1.1 Magnetic confinement

The need of toroidal confinement can be understood by realizing that in a fusion reactor particles must be confined over more than one second and in this time, Hydrogen ions of 10 keV travel over a distance of 1000km or run around a toroidal fusion reactor for 10^{-4} times. Confining these particles in magnetic mirrors has the danger of destroying the mirror effect by collisions and that the particles rapidly escape from the confinement region.

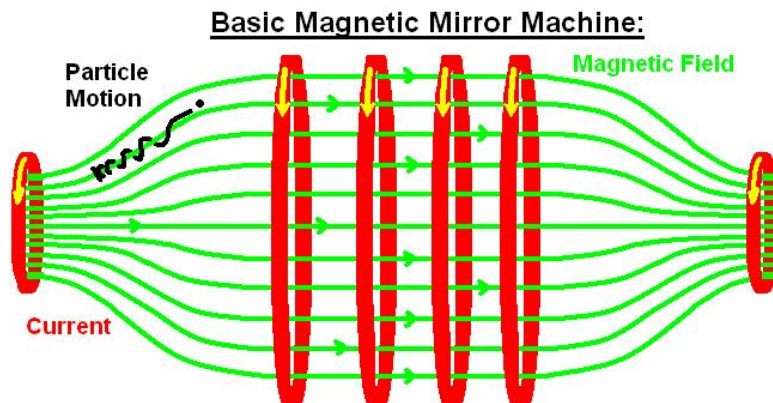


Figure 1.2: Schematic Diagram of Magnetic Mirror

In toroidal confinement one utilizes the tendency of plasma charge particles to gyrate round the magnetic field lines and to follow the toroidal magnetic field lines freely around the torus. In a simple toroidal field with closed field lines one could confine these charge particles if there were no magnetic drift. In the toroidal devices, due to curvature effect and inhomogeneity of magnetic field, \mathbf{B} , the charge particles do not stay on the field lines, instead, they drift in the direction perpendicular to \mathbf{B} and ∇B

$$v_D = \frac{v_{\perp}^2}{2\pi} \frac{\mathbf{B} \times \nabla \mathbf{B}}{B^2} + \frac{u^2}{\Omega} \frac{\mathbf{B} \times (\mathbf{B} \cdot \nabla) \mathbf{B}}{B^3} \quad (1.5)$$

with $\Omega = eB/mc$ is the gyro frequency, v_{\perp} and u are the guiding center velocities perpendicular and parallel to magnetic field respectively. Due to

this drift the particles rapidly escape from the confinement volume. The idea of spitzer was to shape the magnetic field in such a way that inspite of this drift the particles stay inside the vacuum chamber. Under ideal conditions the particles should stay on the toroidal closed surfaces defined by $v_D \cdot \nabla \psi_D = 0$. Those particles which circulate around the torus do not change sign of parallel velocity and since the gyro radius is very small (of the order of mm) the drift surfaces of the circulating particles only deviate little from magnetic surfaces which are defined by $\mathbf{B} \cdot \nabla \psi = 0$. Therefore, particles in the toroidal devices are confined by toroidally closed magnetic surfaces.

Plasma is a collection of charged particles and hence their motion is affected by the electric and magnetic fields. In the past few decades, various devices with magnetic fields have been used to confine hot plasmas for controlled nuclear fusion. These include the stellarator, mirror and tokamak configurations. Confinement in a linear mirror field has advantage over a toroidal system with respect to stability and anomalous diffusion across the field. However, the end losses due to particles leaving along the magnetic field makes this one less attractive for the fusion studies. Since the confinement time plays one of the crucial roles in determining the viability of a fusion reactor, the toroidal system is widely accepted as being the most successful.

Tokamak is one of the toroidal devices used to hold fusion plasmas. It is characterised by a major radius R_0 , a minor radius a , plasma current I_p and an externally produced toroidal magnetic field B_0 . A typical tokamak device is shown in Fig 1.3. In a purely toroidal field, ions and electrons drift in opposite directions because of gradient in the toroidal magnetic field. This charge separation generates an electric field which in turn destroys the confinement through $\mathbf{E} \times \mathbf{B}$ drift. Such a charge separation is avoided by having a poloidal magnetic field (B_p) along with the toroidal one. In tokamak this poloidal field is produced by the plasma itself. But this current carrying plasma column tries to expand in the major radial direction because of hoop force. This has to be balanced by an external vertical magnetic field B_z to maintain equilibrium as shown schematically in Fig 1.3. Such an equilibrium produces nested magnetic surfaces that reduce transport of particles and energy towards the boundary.

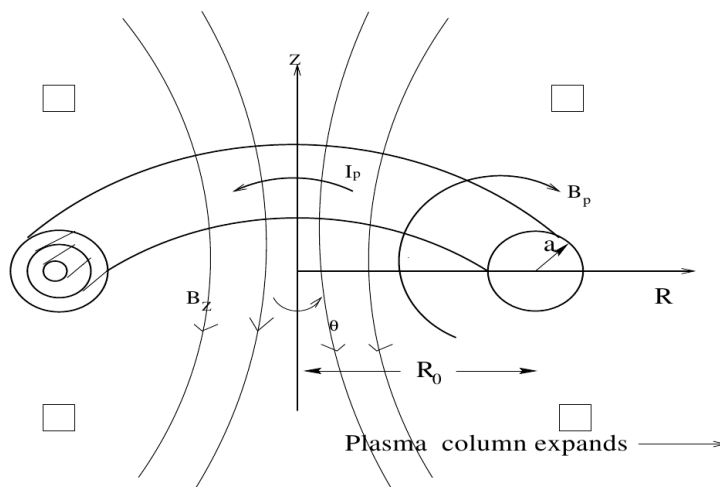


Figure 1.3: Tokamak equilibrium

1.1.2 The tokamak concept

the word tokamak derived from the russian words for 'toroidalnaya kamera magnitnaya katuschka'(toroidal magnetic chamber). Its origin came by attempting to bend a linear pinch into a torus and to maintain the toroidal plasma current by inducing a toroidal loop voltage. An external transformer primary coils are required in tokamak with the plasma acting as the secondary windings. A strong toroidal magnetic field is required for the plasma stability. Unfortunately, a pure toroidal field is not homogenous and curvature and gradient of magnetic field lines lead plasma particles to drift in perpendicular directions. The resulting electric field by charge separation due to the drift is also perpendicular and causes an outward $E \times B$ drift motion of the plasma. This outward drift is avoided by generating a helical magnetic field lines so that each field line passes the upper and lower part of the torus. A combination of toroidal and poloidal magnetic field coils are used to form such a configuration in tokamak. The toroidal plasma current has the natural tendency of an outward radial expansion in the direction of major radius due to hoop force. In earlier tokamaks, this was prevented by a conducting shell surrounding the plasma by the induced image currents on it. In modern tokamaks this is achieved by superimposing a vertical magnetic field which provides more control on the position and the vertical stability of the plasma column.

The magnetic structure in a tokamak consists of various toroidal flux surfaces (magnetic surfaces) and the twist of magnetic field lines in each surface is defined by safety factor, $q(= \frac{\Delta\phi}{2\pi})$, where $\Delta\phi$ is change in toroidal angle by

travelling a full poloidal rotation when following the magnetic field line. If magnetic field lines join up on itself by m toroidal and n poloidal rotations the safety factor is defined by $q=m/n$. The rational q surfaces play an important role in tokamak stability.

Recent tokamak experiments suggest that plasma shape influences the properties of plasma stability and transport. More shaped plasmas have been shown better plasma properties than circular plasmas. Therefore, many additional poloidal field coils are used in recent tokamaks to shape plasmas.

Two techniques are used to separate the plasma from the vacuum vessel. The first is to define a plasma boundary by a material limiter while the second keeps the plasma particles away from the vessel by means of modification of magnetic field to produce the divertor configuration. It has been shown in experiments that divertor plasmas are much more pure than limiter plasmas because divertor plates are far away from the hot plasma region and these plates are capable to handle the heat flux.

The toroidal plasma current also heats the plasma due to its resistivity, η . However, the plasma resistivity η , decreases with the plasma electron temperature as $T_e^{3/2}$ and the current density is limited by plasma instabilities. Therefore, plasma heating by the primary winding (called Ohmic transformer) becomes inefficient after a certain plasma temperature. To achieve plasma temperature of the fusion reactor scale one requires additional heating techniques. This heating can be performed by launching electromagnetic waves into the plasma which can be absorbed either by the ions or the electrons or by injecting highly energetic neutral particles into the plasma.

1.1.3 The tokamak

It is mentioned above that the tokamak uses powerful magnetic fields to isolate the plasma from the walls of the containment vessel thus enabling the plasma to be heated to temperatures in excess of 10 keV. We shall now give a brief description of the device. The tokamak has the following major components

1. The toroidal field (B_ϕ) is around the torus. This is maintained by the toroidal field coils surrounding the vacuum vessel as shown in fig.1.3. In big machines these field coils are built from superconducting materials so that it can carry large amount of current without dissipation to produce a large toroidal magnetic field.

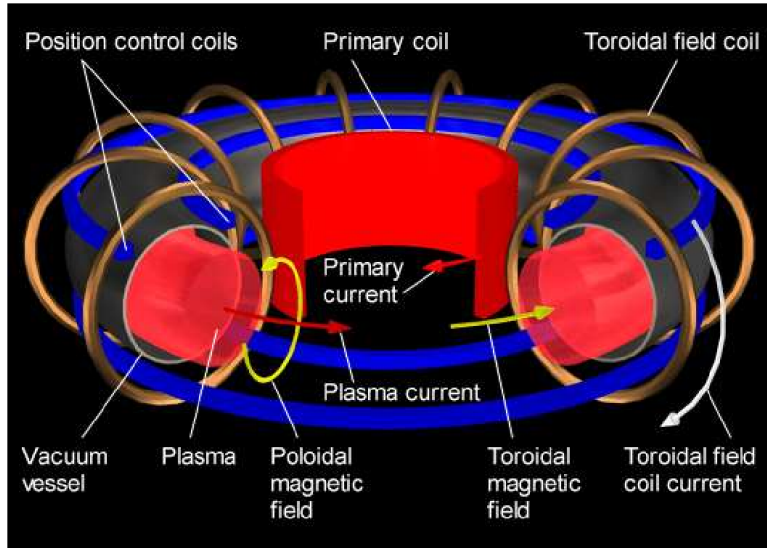


Figure 1.4: Essential constituents of torus shaped magnetic confinement system

2. the poloidal field (B_θ) it is around the plasma cross-section. It pinches the plasma away from the walls and maintains the plasma shape and stability. The poloidal field is induced both internally, by the current driven in the plasma and externally by coils that are positioned around the perimeter of the vessel.

The typical toroidal and poloidal magnetic fields variations in a tokamak are shown in Fig.1.4. The main plasma current in a tokamak machine is induced by the action of a large transformer. A current is passed through the primary coils of the transformer in the center of the torus, which induces a flux change through the torus and produces a toroidal electric field that drives the plasma current. In the case of JET (Joint European Torus) tokamak, the plasma current is about 7 Mega Ampere (MA). The plasma shape and position are further controlled by additional toroidal currents in suitably placed coils. It is to be noted that currently JET is the largest tokamak in the world although the future ITER machine that is under design will be even larger. A cutway diagram of the JET tokamak is shown in Fig.1.5.

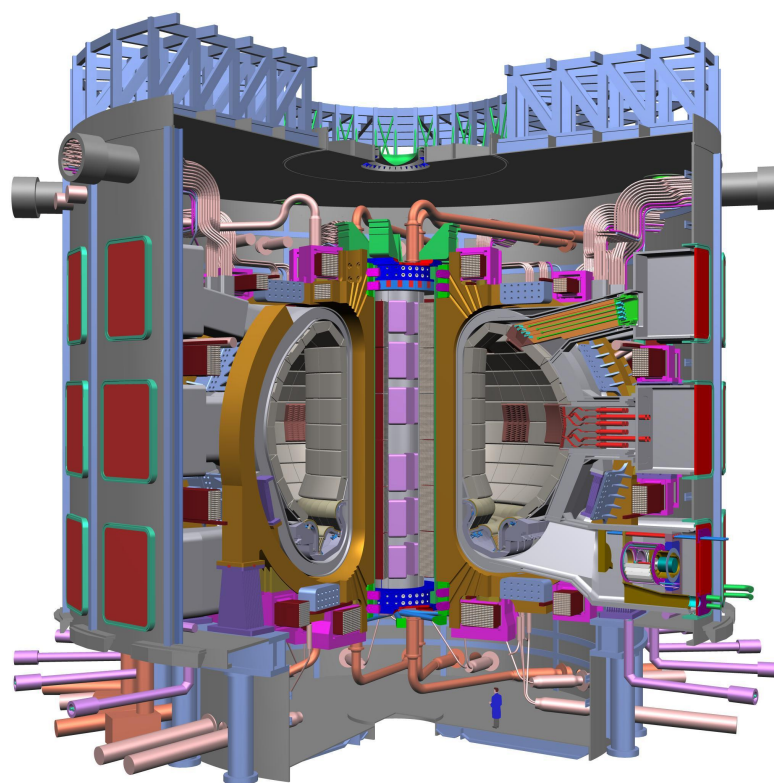


Figure 1.5: Cutway Diagram of Proposed ITER

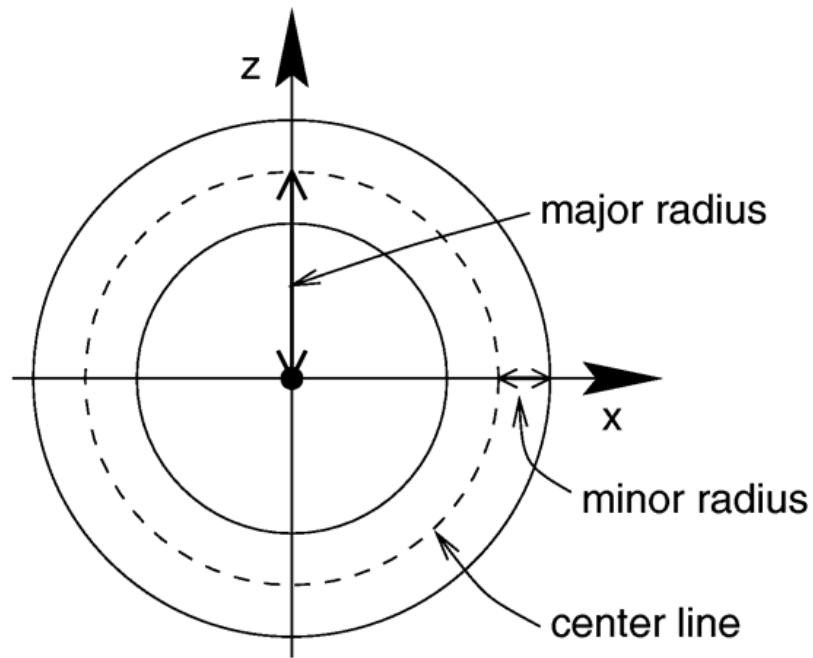
Chapter 2

Theory

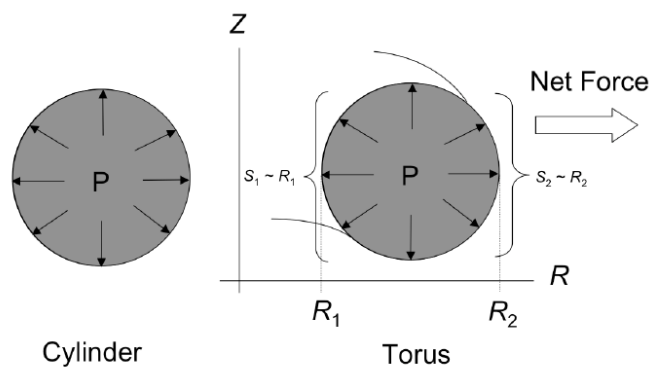
In tokamak ionised gas particles known as plasma (vaguely) collide with each other and fuses whose kinetic energy get increased by induced electric field through central solenoid situated at the axis of tokamak and guided by toroidal and poloidal field coils. Before the tokamak there was magnetic mirror where particle used to get confine in the container. The achievement of MHD equilibrium was possible because of in ideal MHD the fluid can not flow freely across the magnetic field. However, the fluid (or plasma), can flow freely along the field and this allows the fluid to exit the apparatus through the ends of the cylinder. These inherent end losses have proven to be detrimental to achieving fluid confinement in finite cylindrical geometry.

An ingenious solution to the end loss problem is to connect the ends of the cylinder to each other, this transforming the cylinder into a torus (that is tokamak) thus The end losses are completely eliminated moreover all the magnetic field lines remain within the boundaries of the system.

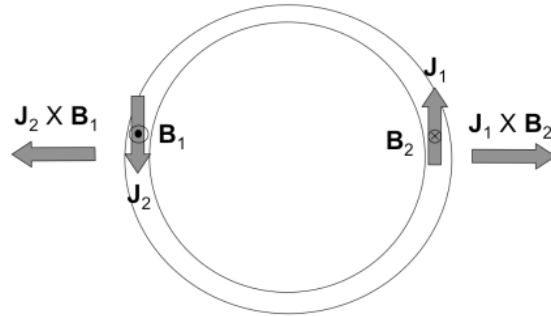
We are thus motivated to study equilibrium in a toroidal configuration. With a torus, it is usual to work in a cylindrical coordinate system (R, ϕ, Z) in which the cross-sectional area of the fluid lies in the (R, Z) plane (the *poloidal plane*) and ϕ is the angle of rotation about Z -axis. The important in which all quantities independent of ϕ is called *axisymmetric*. This is equivalent of Z -independence (or translational symmetry) in the straight cylinder. The radius of the center of poloidal cross-section is called the major radius. The radius of the outer boundary with respect to the major radius is called the minor radius which is shown in figure ?? Unfortunately when a cylindrical MHD equilibrium is bent into a torus it is no longer an equilibrium. Instead it tends to expand outward in the major radial direction. There are two reasons for this. First, a straight cylinder is symmetric about its central



axis. The pressure force are distributed equally on all parts of the outer boundary. However, in a torus the outer part of the surface has a larger surface area ($S_2 R_2$) than the inner surface ($S_1 R_1$) as shown in the figure ??

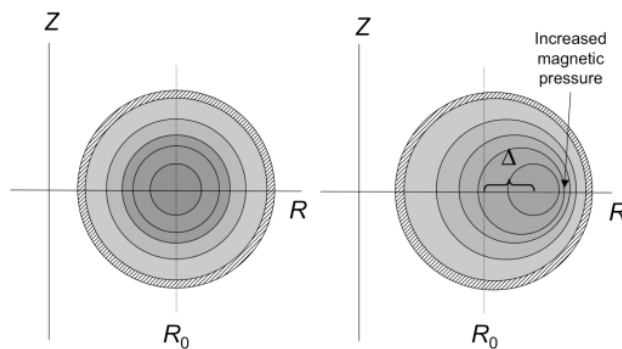


Second, just as parallel currents attract each other by means of the Lorentz force whereas anti-parallel currents repel each other. Each current element at angular location ϕ repels (and is repelled by) the current element at angular location $\phi + \pi$. This results in a net outward force in the radial (R) direction, as shown in the figure ??



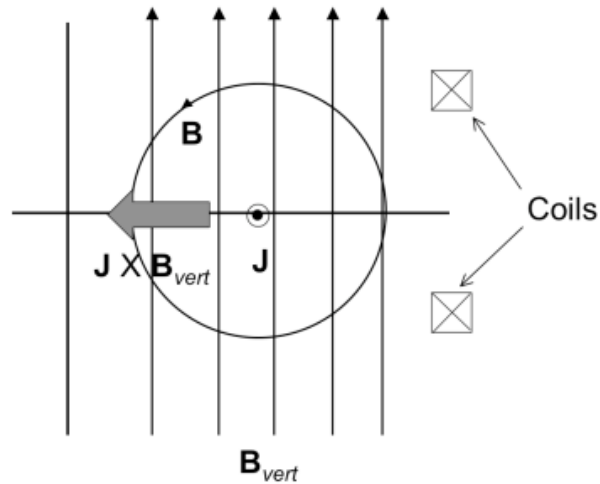
Each of these forces makes the torus expand in major radius. Some externally supplied currents and fields are necessary for equilibrium to be maintained. The system is now finite in extent and the virial theorem applies.

One way to provide these required external fields is to enclose the minor cross section of the torus in an electrically conducting shell. If the shell is a perfect conductor, then as the toroidal fluid tries to expand outward the field lines enclosing the fluid will not be able to penetrate the shell and they will be compressed between the fluid and the shell along the outer (in major radius) part of the torus (called the *outboard side*). This will appear as an increase in magnetic pressure on the outboard side thus opposing the expansion. A new state of equilibrium will be reached in which the fluid is shifted outward with respect to the geometric center line, the magnetic axis (the center of concentric poloidal field) no longer coincides with geometric axis. This is called the *Shafranov shift*, and its magnitude usually denoted by Δ Shown



in figure ??

Another way to provide the external field necessary for toroidal equilibrium is with current carrying Helmholtz coils that induce a field in the Z-direction. If properly oriented this field can interact with the toroidal current (J_ϕ) in the fluid to provide an inward Lorentz force that balances the outward expanding tendency of the torus as shown in the figure ??



Note that the effect of vertical field is to amplify the field due to the plasma current on the outboard side and decrease the field on the inboard side. It thus provides the same mechanism as the conducting shell. In the former case the vertical field is produced by image currents flow in the shell.

In order to proceed beyond these simple cartoons we will have to develop some more general ideas about toroidal equilibria. From now on we will assume that the configurations are axisymmetric, i.e all quantities are independent of the toroidal angle ϕ .

We have seen that in a straight (infinitely long) cylinder the pressure is constant on concentric cylindrical surfaces i.e, $p=p(r)$. Since $\nabla p = \mathbf{J} \times \mathbf{B}$, we have $\mathbf{B} \cdot \nabla p = 0$ that the pressure is constant along the direction of \mathbf{B} . Conversely the field lines of \mathbf{B} must lie in constant pressure surfaces, i.e, they must wrap around a cylindrical surface. Since $\mathbf{J} \cdot \nabla p = 0$ also, the current must also lie in these surfaces. However, it need not be aligned with \mathbf{B} if there is a pressure gradient across these surfaces there will be a

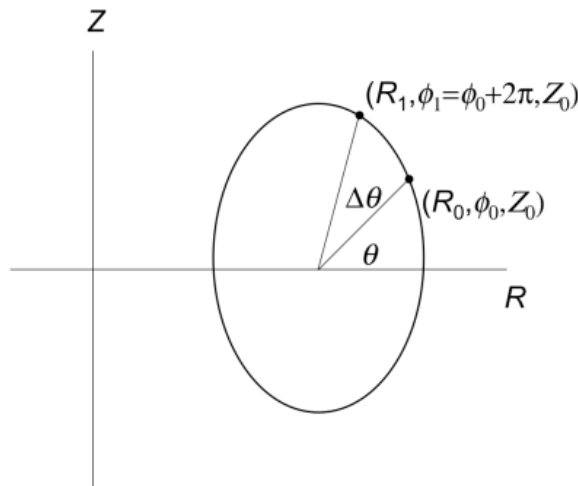
component perpendicular to \mathbf{B} also with in the constant pressure surface that is given by $\mathbf{J}_\perp = \mathbf{B} \times \nabla p / B^2$.

In an axisymmetric torus these constant pressure surfaces are shifted outward with respect to each other as discussed above. They form nested toroidal surfaces. However since $\mathbf{B} \cdot \nabla p = 0$ the magnetic field lines must still lie completely within these surfaces. These are called flux surfaces and can be called 'labelled' by any variable that is constant on them e.g. the pressure, different surfaces can be identified by their value of pressure.

The equations for a field line in cylindrical geometry are

$$\frac{dR}{B_R} = \frac{Rd\phi}{B_\phi} = \frac{dZ}{B_Z} \quad (2.1)$$

Consider a field line that begins at coordinates (R_0, ϕ_0, Z_0) . This point will make an angle θ_0 with respect to the center of the concentric surfaces of constant pressure. Now integrate this field line once around the torus i.e. follow its trajectory until $\phi_1 = \phi_0 + 2\pi$. In general this will intersect the poloidal plane at R_1 and Z_1 , which are in general different from R_0 and Z_0 and which make different angle $\theta_0 + \Delta\theta$ with respect to the axis. This field line can be said to map the point (R_0, Z_0) into the point (R_1, Z_1) as shown



in figure ??

We know that the pressure at (R_1, Z_1) must be the same as the pressure at point (R_0, Z_0) . There are two possible types of trajectory (or mapping)

for a given field line. One is that it fills the entire volume ergodically. In that case the pressure must be constant throughout volume. This is not consistent with confinement while this can occur dynamically during the evolution of the magnetoplasma system we will not consider it as part of our discussion of equilibrium. The second case is that the field line maps out a two dimensional surface which corresponds to a constant pressure surface. Then there are two further possibilities. The first is that the field line while remaining on the surface nonetheless never returns to its original position. These field lines fill the two dimensional surface ergodically but they do not close upon themselves. Surfaces on which the field lines are ergodic are said to be irrational. The second possibility is that the field line returns exactly to its initial coordinates (closes upon itself) after N turns around the torus. These surfaces are said to be rational.

These concepts can be quantified by introducing the *rotational transform*

$$i = \lim_{N \rightarrow \infty} \frac{1}{N} \sum_{n=1}^N \Delta\theta_n \quad (2.2)$$

Where $\Delta\theta_n$ is the change in the angle θ during the n^{th} toroidal circuit. If $i/2\pi$ is a rational number, then the field line is closed and the surface is rational. Otherwise, the field line is not closed and the surface is irrational. If i is rational number, it is the number of times the field line must transit the torus in the toroidal ϕ direction for it to make one complete transit one complete transit about the surface in the poloidal (R, Z) plane. The quantity $q \equiv 2\pi/i$ is called the safety factor. It is important in the theories of equilibrium and stability of confined plasmas.

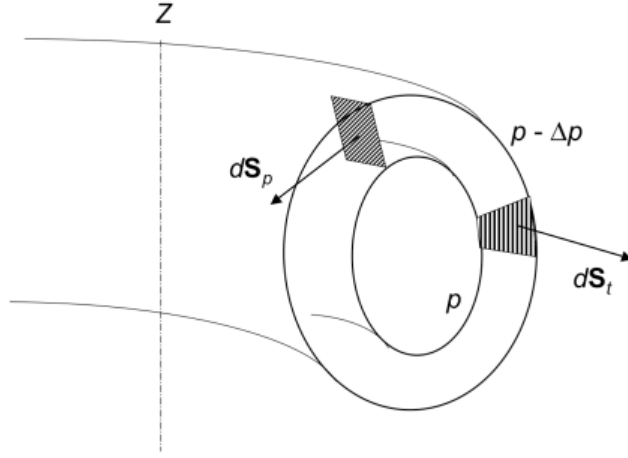
It is possible to define fluxes based on the poloidal field (i.e B_R and B_Z) and toroidal field (B_ϕ) components. We define $d\mathbf{S}_t$ and $d\mathbf{S}_p$ as surface elements extending between constant pressure surfaces oriented in the toroidal and poloidal directions respectively as shown in the figure ??

The poloidal flux is defined as

$$\psi_p(p) = \int \mathbf{B} \cdot d\mathbf{S}_p \quad (2.3)$$

Since ψ_p is a function of the pressure we can adopt ψ_p as a surface label. (Any function $f(p)$) that is constant on a flux surface is called a *surface function* can equally well be adopted as a surface label). We define the toroidal flux as

$$\psi_t(p) = \int \mathbf{B} \cdot d\mathbf{S}_t \quad (2.4)$$



It is useful to also define the *toroidal current*

$$I_t(p) = \int \mathbf{J} \cdot d\mathbf{S}_t \quad (2.5)$$

and the poloidal current

$$I_p(p) = \int \mathbf{J} \cdot d\mathbf{S}_p \quad (2.6)$$

Since these are all functions of the pressure they are all surface functions and could serve as surface labels. Finally we can define the volume combined within a constant pressure surface. It is often useful to use the coordinate system as shown in figure ??

The coordinates of a point can be equally well written as (R, Z) or (r, θ) where

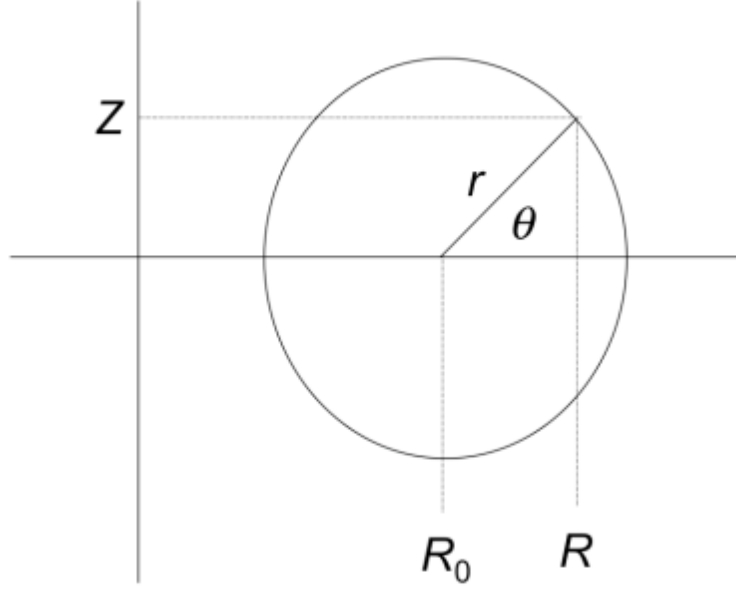
$$R = R_0 + r \cos \theta \quad (2.7)$$

and

$$Z = r \sin \theta \quad (2.8)$$

Then $\psi_p(r, \theta) = \text{constant}$ defines a flux surface. We assume that an inverse transformation exists (although it may be difficult to compute) i.e. the radius of a flux surface is given by $V(\psi) = \int_0^{2\pi} d\phi \int_0^{2\pi} d\theta \int_0^{r(\theta, \psi)} (R_0 + r \cos \theta) r dr$ We now proceed to derive the equation that describe axially symmetric force balance in a torus.

1. $\nabla \cdot \mathbf{B} = 0$
2. Ampere's law, $\mu_0 \mathbf{J} = \nabla \times \mathbf{B}$ and



3. Force balance, $\nabla p = \mathbf{J} \times \mathbf{B}$

1. $\nabla \cdot \mathbf{B} = 0$ The total magnetic field is $\mathbf{B} = \mathbf{B}_p + B_\phi \hat{e}_\phi$ where \mathbf{B}_p is the poloidal field containing the R and Z components. Since the system is independent of ϕ we have

$$\frac{1}{R} \frac{\partial}{\partial R} (R B_R) + \frac{\partial B_Z}{\partial Z} = 0 \quad (2.9)$$

Since $\mathbf{B} = \nabla \times \mathbf{A}$ we have

$$B_R = -\frac{\partial A_\phi}{\partial Z} \quad (2.10)$$

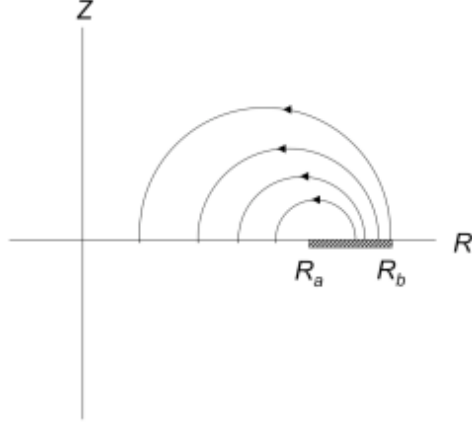
and

$$B_Z = \frac{1}{R} \frac{\partial}{\partial R} (R A_\phi) \quad (2.11)$$

If we define the stream function $\psi = R A_\phi$ then 2.9 will be satisfied automatically. The poloidal field can be expressed as

$$\mathbf{B}_p = \frac{1}{R} \nabla \psi \times \hat{e}_\phi \quad (2.12)$$

The stream function can be related to the poloidal flux by noting that the latter is a measure of the flux of B_Z passing through the midplane of



torus ($Z=0$) between the shifted center of the surfaces R_a and another radius $R_b > R_a$ as shown in the figure ??

Then

$$\psi_p = \int_0^{2\pi} d\phi \int_{R_a}^{R_b} R dB_Z(R, 0) \quad (2.13)$$

$$= 2\pi \int R dR \frac{1}{R} \frac{\partial \psi}{\partial R} \Big|_{Z=0} \quad (2.14)$$

$$2\pi \psi(R_b, 0) \quad (2.15)$$

where we have set $\psi(R_a, 0) = 0$. Therefore we can and will from now on label the flux surface with ψ .

2. *Ampere's law*, $\mu_0 \mathbf{J} = \nabla \times \mathbf{B}$. Using the identities $\nabla \cdot \hat{e}_\phi = 0$, $\nabla \times \hat{e}_\phi = \hat{e}_Z/R$ and $\nabla \hat{e}_\phi = -\hat{\phi} \hat{e}_R/R$ we have

$$\mu_0 \mathbf{J} = \nabla \times \left(\frac{1}{R} \nabla \psi \times \hat{e}_\phi + B_\phi \hat{e}_\phi \right) \quad (2.16)$$

$$= \mu_0 J_\phi \hat{e}_\phi + \frac{1}{R} \nabla (RB_\phi) \times \hat{e}_\phi \quad (2.17)$$

where the toroidal current density is

$$\mu_0 J_\phi = -\nabla \cdot \left(\frac{1}{R} \nabla \psi \right) \quad (2.18)$$

It is customary to define the operator $\Delta^*\psi$ as

$$\Delta^* \equiv R\nabla \cdot \left(\frac{1}{R} \nabla \psi \right) = R \frac{\partial}{\partial R} \left(\frac{1}{R} \frac{\partial \psi}{\partial R} \right) + \frac{\partial^2 \psi}{\partial Z^2} \quad (2.19)$$

so that

$$\mu_0 J_\phi = -\frac{1}{R} \Delta^* \psi \quad (2.20)$$

3. *Force Balance*, $\nabla p = \mathbf{J} \times \mathbf{B}$. Since there is no ϕ dependence we have $\mathbf{B}_p \cdot \nabla p = 0$. Using (2.12) $(\nabla \psi \times \hat{e}_\phi) \cdot \nabla p = 0$ or

$$(\nabla \psi \times \nabla p) \cdot \hat{e}_\phi = 0 \quad (2.21)$$

This expression vanished identically if $p = p(\psi)$ as it must since by construction the pressure is constant on flux surfaces.

Similarly since $\mathbf{J} \cdot \nabla p = 0$ it follows from 2.16 that

$$[\nabla (RB_\phi \times \nabla p)] \cdot \hat{e}_\phi = 0 \quad (2.22)$$

so that $RB_\phi F(\psi)$ which we could not anticipate. The function $F(\psi)$ is related to the total poloidal current (plasma plus coil) flowing between the major axis of the torus $R = 0$ and any radius R_b :

$$\begin{aligned} I_p &= \int \mathbf{J}_p \cdot d\mathbf{S} \\ &= \int_0^{2\pi} d\phi \int_0^{R_b} R dR J_Z(R, 0) \\ &= 2\pi \int_0^{R_b} R dR \frac{1}{R} \frac{\partial}{\partial R} (RB_\phi) \Big|_{Z=0} \\ &= 2\pi RB_\phi(R_b, 0) \\ &= 2\pi F(\psi) \end{aligned} \quad (2.23)$$

The expression for force balance $\nabla p = \mathbf{J} \times \mathbf{B}$ is then

$$p' \nabla \psi = \left(J_\phi \hat{e}_\phi + \frac{1}{R\mu_0} F' \nabla \psi \times \hat{e}_\phi + B_\phi \hat{e}_\phi \right) \quad (2.24)$$

where $(..)'$ denotes differentiation with respect to ψ . After some vector algebra this becomes

$$p' = -\frac{1}{\mu_0 R^2} (\Delta^* \psi + FF') \quad (2.25)$$

or

$$\Delta^* \psi = -\mu_0 R^2 p' - FF' \quad (2.26)$$

Equation 2.26 is called the *Grad-Shafranov equation*. It is one of the most famous equation arising from MHD. It is a second order partial differential equation that given the functions $p(\psi)$ and $F(\psi)$, describes equilibrium in an axisymmetric torus. The functions $p(\psi)$ and $F(\psi)$ are completely arbitrary and must be determined from considerations other than theoretical force balance.

At least in principal, given the functions $p(\psi)$ and $F(\psi)$ along with the appropriate boundary conditions (generally that ψ is specified on some boundary) Equation 2.26 can be solved for $\psi(R, Z)$. This gives the equilibrium flux distribution. However it is important to note that functions p and F can be (and generally are) nonlinear so that these solutions are not guaranteed to either exist or to be unique, there may be no solution or many solutions satisfying both (2.26) and boundary conditions.

As an example of the character of the solutions of the Grad-Shafranov equation, we consider the linear case $F=\text{constant}$ ($F' = 0$) and

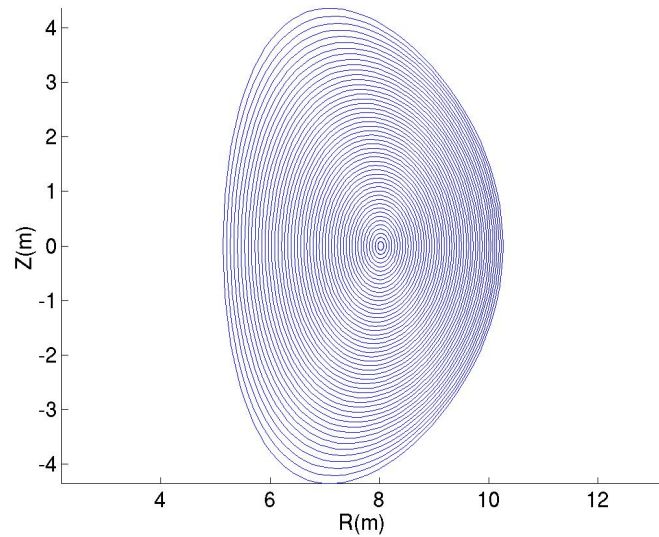
$$p' = \text{constant} = \frac{8\psi_0}{\mu_0 R_0^2} (1 + \alpha^2) \quad (2.27)$$

where $\psi_0 = \psi(R_0, 0)$ and α is a constant. Then it can be verified that the solution of the equation 2.26 is

$$\psi(R, Z) = \frac{\psi_0 R^2}{R_0^4} (2R_0^2 - R^2 - 4\alpha^2 Z^2) \quad (2.28)$$

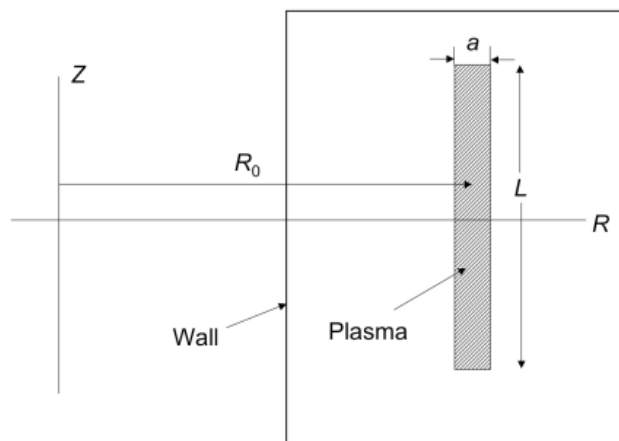
Surfaces of constant ψ for $\alpha = 1$ are shown in the figure ??

The flux surfaces are closed and nearly circular near the magnetic axis at R_0 . They remain closed by become non-circular shaped when $\psi/\psi_0 > 0$ and become open when $\psi/\psi_0 < 0$. The surface $\psi/\psi_0 = 0$ is called a separatrix, it separates the regions of closed an open flux surfaces. The constant α determines the shape of the closed flux surfaces. As α increases from 1 they become more elongated and vice versa. The boundary of the plasma is defined as $p = 0$. The function $p(\psi)$ can be adjusted by adding a constant so that any surface $\psi/\psi_0=\text{constant}$ can be the boundary. Finally since $F=\text{constant}$, $B_\phi \propto 1/R$



Since the Grad-Shafranov equation is nonlinear there are no general existence or uniqueness proofs available. There may be one solution, no solutions or multiple solutions depending on the specific forms of $p(\psi)$ and $F(\psi)$. Points in parameter space where solutions coalesce or disappear are called bifurcation points. I would present a specific example of this behavior.

Consider the case of a tall thin toroidal plasma with large aspect ratio. The plasma is surrounded by a conducting wall as shown in figure ??



We assume $R_0 \gg a$ and $L \gg a$ and write $\Delta^*\psi$ as

$$\Delta^*\psi = \frac{\partial^2\psi}{\partial R^2} - \frac{1}{R} \frac{\partial\psi}{\partial R} + \frac{\partial^2\psi}{\partial Z^2} \quad (2.29)$$

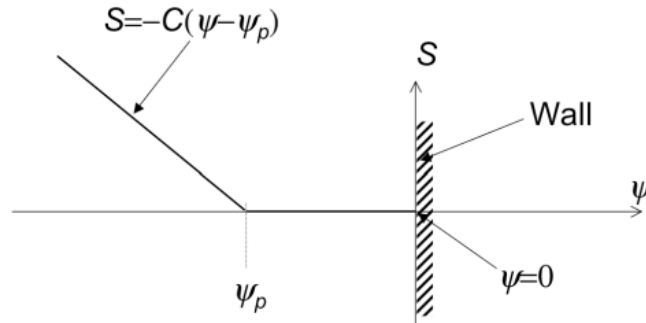
Since R only varies relatively slightly within the plasma we have $\partial/\partial R \sim 1/a$, $(1/R)\partial/\partial R \sim 1/aR_0$ and $\partial/\partial Z \sim 1/L$. Then to lowest order, $\Delta^*\psi \approx \partial^2\psi/\partial R^2$ and equation (2.26) becomes

$$\frac{d^2\psi}{dR^2} = -\mu_0 R^2 p' - FF' = -S' \quad (2.30)$$

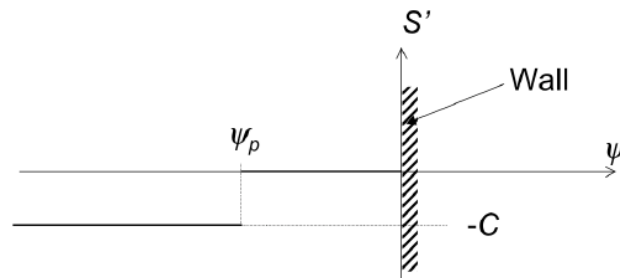
Where $S(\psi) = \mu_0 R^2 p(\psi) + F^2(\psi)/2$ is a nonlinear function of ψ here chosen to be

$$S(\psi) = -C(\psi - \psi_p) \quad \text{for } \psi < \psi_p \\ = 0 \quad \text{otherwise} \quad (2.31)$$

The flux at the plasma boundary is ψ_p and the flux at the wall is zero ψ is negative everywhere; C is constant. This is sketched in the figure ??



The function S' is sketched in the following figure ??



Now let $x = R - R_0$. Then Equation 2.31 is

$$\frac{d^2\psi}{dx^2} = 0 \quad \psi > \psi_p \quad (2.32)$$

$$= C \quad \psi < \psi_p \quad (2.33)$$

In the vacuum region, $\psi > \psi_p$, the solution is

$$\psi_{>} = \alpha x + \beta \quad (2.34)$$

and in the plasma $\psi < \psi_p$, the solution is

$$\psi_{<} = \frac{1}{2}Cx^2 + \gamma x + \delta \quad (2.35)$$

Let the wall be located at $x_{wall} = R_{wall} - R_0$. The solution must satisfy the boundary condition $\psi_{>} = 0$ at $x = x_{wall}$. Since Equation 2.32 is symmetric in x , the solution must be symmetric about $x = 0$. The solution must be continuous at $x = x_p$. Further, $B_z = d\psi/dx$ must be continuous across the boundary of the plasma at $x = x_p$. The solution profile is sketched in the

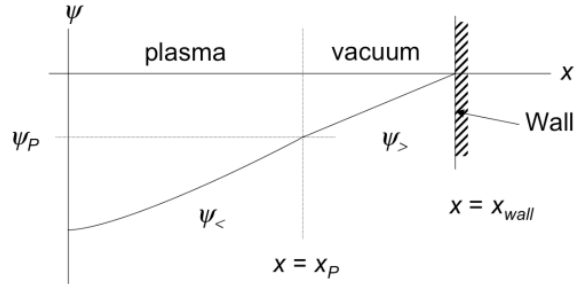


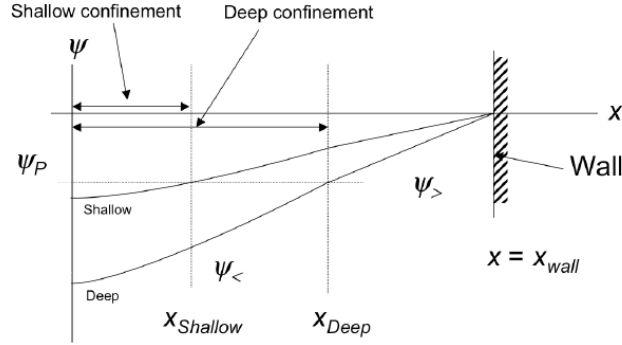
figure ??

Combining these conditions yields a quadratic equation for the location of the plasma boundary x_p whose solution is

$$x_p = \frac{x_{wall}}{2} \left[1 \pm \sqrt{1 - \frac{4|\psi_p|}{x_{wall}^2 C}} \right] \quad (2.36)$$

There are two possible solutions for the location of the plasma/vacuum boundary. The solution associated with the positive sign is called the deep solution and the solution associated with the negative sign is called the shallow solution. These are sketched below ??

In the shallow solution, the plasma is confined in the region $0 \leq x \leq x_{shallow}$. For the deep solution the confinement region is $0 \leq x \leq x_{shallow}$.



From equation 2.36 we see that when $4|\psi_p|/x_{wall}^2 C > 1$ there are no real solutions and equilibrium is impossible. This occurs when

$$C < \frac{4|\psi_p|}{x_{wall}^2} \quad (2.37)$$

The quantity $C_0 = 4|\psi_p|/x_{wall}^2$ is called the bifurcation point for the equilibrium. Above this value of C there are two solutions. These solutions merge at the bifurcation. For values of C below the bifurcation point there are no solutions. When $C \rightarrow \infty, x_{deep} \rightarrow x_{wall}$ and $x_{shallow} \rightarrow 0$ so that the deep solution survives.

Chapter 3

Methods

3.1 Introduction

For transport simulations of high beta (poloidal betas on order of the aspect ratio), non circular tokamak plasmas, it is important to have a computationally fast, yet sufficiently accurate method for determining the flux surface geometry. Repeatedly solving the two dimensional grad-shafranov equation for evolving flux surface geometry can significantly increase the computer time and storage requirements of a transport code. Variational method to find approximate solutions to the grad-shafranov equation is studied which is computationally efficient. The flux surface coordinates (R, Z) are expanded in Fourier series in a poloidal angle θ . Through the use of variational method the Fourier amplitudes of R and Z are obtained by solving a set of coupled ordinary differential equations, which are moments of Grad-Shafranov equation. The approximation of flux surface geometry obtained in this way is sufficiently accurate for transport simulations and may also be used to evaluate magnetohydrodynamic stability criteria.

3.2 Analytical formulation of the inverse equilibrium problem

3.2.1 Coordinate transformation

In considering a two-dimensional axisymmetric toroidal system with nested magnetic surfaces, It is convenient to transform the cylindrical coordinates (R, Z) to the flux surface representation (ρ, θ) where $\rho = \rho(\psi)$ is a flux surface label, θ is a poloidal angle that increases by 2π the short way around the torus and ψ is poloidal magnetic flux enclosed between the flux surface $\rho(\psi)$

and the axis of symmetry. The angle θ is arbitrary except that Jacobian of the transformation is finite. Assuming that the flux surfaces up-down symmetry [$Z(\rho, \theta) = -Z(\rho, -\theta)$] it is possible to represent the coordinate transformation as a Fourier series in θ

$$R(\rho, \theta) = \sum_{n=0}^{\infty} R_n(\rho) \cos n\theta \quad (3.1)$$

$$Z(\rho, \theta) = \sum_{n=1}^{\infty} Z_n(\rho) \cos n\theta \quad (3.2)$$

The amplitudes $R_0(\rho)$, $R_1(\rho)$ and $Z_1(\rho)$ describe the shift the minor radius and the ellipticity of the flux surfaces respectively whereas the amplitudes $R_2(\rho)$ and $Z_2(\rho)$ describe the triangularity of the flux surfaces.e.g If only the amplitudes $R_0(\rho)$, $R_2(\rho)$ and $Z_1(\rho)$ are retained, the flux surfaces are shifted ellipses.

3.2.2 Variational principle

The fourier series for R and Z may be substituted into the Grad-shafranov equation expressed in (ρ, θ) coordinates (the inverse of the grad-shafranov equation) to yield an infinite system of coupled ordinary differential equations for the expansion coefficients. In practice, only a finite number N of amplitude functions will be retained to obtain an approximate solution for the flux surface geometry. Since the inverse grad-shafranov equation is non linear in R and Z , the resulting harmonic coupling generally yields (for finite N) more equations than the number of fourier amplitudes. Therefore a method must be determined for selecting the appropriate linear combination of these equations that will yield the best approximate solution. A variational principle now be introduced from which the optimum ordinary differential equations for the fourier amplitudes of the inverse mapping may be obtained. A related approach has been developed by halt and applied to particular case of shifted elliptical surfaces.

Consider the Grad-shafranov equation

$$\Delta^* \psi(R, Z) = -(8\pi^2 R) J_\phi \quad (3.3)$$

where J_ϕ is the toroidal component of the current density

$$J_\phi = 2\pi c R \left[p'(\psi) + FF'(\psi)/\pi c^2 R^2 \right] \quad (3.4)$$

F is the poloidal current enclosed between the axis of symmetry and the magnetic surface of interest and

$$\Delta^* \psi(R, Z) = R^2 \nabla \cdot \left(\frac{\nabla \psi}{R^2} \right) = \frac{\partial^2 \psi}{\partial R^2} - \frac{1}{R} \frac{\partial \psi}{\partial R} + \frac{\partial^2 \psi}{\partial Z^2} \quad (3.5)$$

Where $p'(\psi) = dp/d\psi$ and $F'(\psi) = dF/d\psi$
Now consider the volume integral

$$Q = \int_V dR dZ L(\psi, \psi_R, \psi_Z, R) \quad (3.6)$$

Where $\psi_R = \partial\psi/\partial R$, $\psi_Z = \partial\psi/\partial Z$ and L is lagrangian

$$L = R \left(\frac{B_p^2}{8\pi} - \frac{B_t^2}{8\pi} - p(\psi) \right) \quad (3.7)$$

and integration is over entire plasma volume V .

Here B_p and B_t are poloidal and toroidal magnetic field components, respectively

$$B_p = |\nabla \psi|/2\pi R \quad (3.8)$$

$$B_t = 2F(\psi)/cR \quad (3.9)$$

Using the fact that operator $R^{-2}\Delta^*$ is self adjoint it may be shown that Q is stationary with respect to variations of ψ although subject to constraint $\delta\psi=0$ for satisfying the grad-shafranov equation. Conversely, the euler equation

$$\frac{\partial L}{\partial \psi} - \frac{\partial}{\partial R} \frac{\partial L}{\partial \psi_R} - \frac{\partial}{\partial Z} \frac{\partial L}{\partial \psi_Z} = 0 \quad (3.10)$$

Which reproduces the grad-shafranov equation. Note that $B_p^2/8\pi \propto |\nabla\psi|^2$ plays the role of kinetic energy in eq 3.7 and $B_t^2/8\pi + p(\psi)$ is effective potential energy. Indeed, the Hamiltonian corresponding to the Lagrangian L is proportional to the total energy in the equilibrium system.

Now consider the transformation in eq 3.6 of the independent (integration) variables (R, Z) to (ρ, θ) coordinates

$$Q = \int_0^a \int_0^{2\pi} d\rho d\theta \tilde{L}(R, R_\rho, R_\theta, Z_\rho, Z_\theta, \psi, \psi_\rho) \quad (3.11)$$

Here $\rho = a$ denotes the outermost flux surface and the subscripts ρ and θ denote the differentiation with respect to these variables . The transformed lagrangian is

$$\tilde{L} = \sqrt{g} \left(\frac{1}{32\pi^3} \frac{g_{\theta\theta}}{g} [\psi'(\rho)]^2 - \frac{F^2(\psi)}{2\pi c^2 R^2} - p(\psi) \right) \quad (3.12)$$

Where \sqrt{g} is the Jacobian of the transformation from (R, ϕ, Z) to (ρ, θ, ϕ) coordinates ϕ is ignorable toroidal angle

$$\sqrt{g} = R\tau \quad (3.13)$$

$$\tau = R_\theta Z_\rho - R_\rho Z_\theta \quad (3.14)$$

and $g_{\mu\nu}$ for $(\mu, \nu) \in (\rho, \theta)$ are the elements of the metric tensor

$$g_{\mu,\nu} = R_\mu R_\nu + Z_\mu Z_\nu \quad (3.15)$$

and

$$g_{\phi\phi} = R^2 \quad (3.16)$$

All other metric elements are zero. In the representation of Q given by eq 3.11, the quantities R , Z and ψ are interpreted as dependent variables.

Unlike the fixed boundary case, the shape of boundary surface is not known but must be determined self-consistently from the currents in the external shaping coils which enter into the problem through the boundary condition at the outermost flux surface at $\rho = a$

$$\psi(a) = \tilde{\psi}[\tilde{r}(a, \theta)] \quad (3.17)$$

where

$$\tilde{\psi}\tilde{r} = \int d\tilde{r}' G(\tilde{r}/\tilde{r}') J_e(\tilde{r}') + \int_{\Omega_p} d\tilde{r}' G(\tilde{r}/\tilde{r}') J_p(\tilde{r}') \quad (3.18)$$

Where J_e is the toroidal current density due to external shaping coils $\tilde{r} = (R, Z)$, $G(\tilde{r}/\tilde{r}')$ is the Green's function for a toroidal current source.

$$G(\tilde{r}/\tilde{r}') = \frac{4\pi}{c} \frac{(RR')^{1/2}}{\kappa} [(2 - \kappa^2)K(\kappa) - 2E(\kappa)] \quad (3.19)$$

Where $K(\kappa)$ and $E(\kappa)$ are complete integrals, and

$$\kappa^2 = \frac{4RR'}{(R + R')^2 + (Z - Z')^2} \quad (3.20)$$

$G(\tilde{r}/\tilde{r}')$ satisfies the equation

$$\Delta^* G(\tilde{r}/\tilde{r}') = -\frac{8\pi^2 R}{c} \delta(R - R') \delta(Z - Z') \quad (3.21)$$

For a filament distribution of external sources eqn 3.18 reduces to

$$\tilde{\psi}(\tilde{r}) = \sum_{m=1}^M G(\tilde{r}/\tilde{r}'_{em}) I_{em} + \int_{\omega_p} d\tilde{r}' G(\tilde{r}/\tilde{r}') J_p(\tilde{r}') \quad (3.22)$$

Where I_{em} and \tilde{r}_{em} denote the current strength and the position of the m external current filament, respectively. Making use of surface average of the toroidal component of Ampere's law

$$\psi'(\rho) = -\frac{4\pi}{c} \frac{I(\rho)}{\left\langle \frac{g_{\theta\theta}}{g^{1/2}} \right\rangle} \quad (3.23)$$

the relationship $J_p = -c\Delta^*\psi/8\pi^2R$ and equation 3.21, the surface integral appearing in 3.25 may be reduced to a line integral. Here $I(\rho)$ is the toroidal current enclosed by the flux surface ρ . For \tilde{r} outside of Ω_p equation 3.25 may be reduced to

$$\tilde{\psi}(\tilde{r}) = \sum_{m=1}^M G(\tilde{r}/\tilde{r}_{em})I_{em} + \frac{I(a)}{\left\langle \frac{g_{\theta\theta}}{g^{1/2}} \right\rangle|_a} \int_0^{2\pi} \frac{d\theta'}{2\pi} \frac{g_{\theta\theta}(a, \theta')}{g^{1/2}} G[\tilde{r}/\tilde{r}'(a, \theta')] \quad (3.24)$$

And for \tilde{r} inside ω_p equation 3.18 may be reduced to

$$\begin{aligned} \tilde{\psi}[\tilde{r}(\rho, \theta)] &= \frac{4\pi}{c} \int_{\rho}^a d\rho' \frac{I(\rho')}{\left\langle \frac{g_{\theta\theta}}{g^{1/2}} \right\rangle} \\ &+ \sum_{m=1}^M G[\tilde{r}(\rho, \theta)/\tilde{r}_{em}] I_{em} + \frac{I(a)}{\left\langle \frac{g_{\theta\theta}}{g^{1/2}} \right\rangle|_a} \int_0^{2\pi} \frac{d\theta'}{2\pi} \frac{g_{\theta\theta}(a, \theta')}{g^{1/2}} G[\tilde{r}/\tilde{r}'(a, \theta')] \end{aligned} \quad (3.25)$$

Since the surface integral appearing in equation 3.18 is expensive to evaluate numerically. It is advantageous to use 3.24 and 3.25 instead of equation 3.18 to evaluate $\tilde{\psi}(\tilde{r})$

Since Q is scalar, its value must be independent of the particular coordinate representation used in its evaluation. Thus, the form for Q given in eq 3.11 must be stationary with respect to variations of the dependent variables R and Z which are subjected to the free boundary condition the variation of Q with respect to these variables yields

$$\delta Q_R = \int_0^a \int_0^{2\pi} d\rho d\theta \delta R \left(\frac{\partial \tilde{L}}{\partial R} - \frac{\partial}{\partial \rho} \frac{\partial \tilde{L}}{\partial R_\rho} - \frac{\partial}{\partial \theta} \frac{\partial \tilde{L}}{\partial R_\theta} \right) \quad (3.26)$$

$$= - \int_0^a \int_0^{2\pi} d\rho d\theta \delta R R Z_\theta \hat{G} \quad (3.27)$$

and

$$\delta Q_Z = \int_0^a \int_0^{2\pi} d\rho d\theta \delta Z \left(-\frac{\partial}{\partial \rho} \frac{\partial \tilde{L}}{\partial Z_\rho} - \frac{\partial}{\partial \theta} \frac{\partial \tilde{L}}{\partial Z_\theta} \right) \quad (3.28)$$

$$= \int_0^a \int_0^{2\pi} d\rho d\theta \delta Z R R_\theta \hat{G} \quad (3.29)$$

where

$$\hat{G} = \frac{\psi'(\rho)}{16\pi^3 \sqrt{g}} \left[\frac{\partial}{\partial \rho} \left(\frac{g_{\theta\theta}}{\sqrt{g}} \psi'(\rho) \right) - \frac{\partial}{\partial \theta} \left(\frac{g_{\rho\theta}}{\sqrt{g}} \right) \psi'(\rho) \right] + p'(\rho) + \frac{FF'(\rho)}{\pi c^2 R^2} \quad (3.30)$$

Note that $\hat{G} = \psi'(\rho)(16\pi^3 R^2)^{-1}(\Delta^* \psi + 8\pi^2 R J_\phi / c)$ is proportional to the equilibrium operator in 3.3 expressed in (ρ, θ) coordinates. It follows that Q is stationary if $R(\rho, \theta)$ or $Z(\rho, \theta)$ satisfies inverse grad-shafranov equation

$$\hat{G} = 0 \quad (3.31)$$

and that conversely the euler equation

$$\frac{\partial \tilde{L}}{\partial R} - \frac{\partial}{\partial \rho} \frac{\partial \tilde{L}}{\partial R_\rho} - \frac{\partial}{\partial \theta} \frac{\partial \tilde{L}}{\partial R_\theta} = 0 \quad (3.32)$$

or

$$-\frac{\partial}{\partial \rho} \frac{\partial \tilde{L}}{\partial Z_\rho} - \frac{\partial}{\partial \theta} \frac{\partial \tilde{L}}{\partial Z_\theta} = 0 \quad (3.33)$$

reproduces the inverse grad-shafranov equation. The fact that varying either R or Z yields the same eqn 3.31 expresses the arbitrariness of the poloidal angle θ . For example if θ is chosen such that (ρ, θ) coordinates are orthogonal eq 3.31 together with the orthogonality condition $\nabla \rho \cdot \nabla \theta = -\tau^{-2}(R_\rho R_\theta + Z_\rho Z_\theta) = 0$ yield the set of inverse equilibrium equations used by vabischchevich et al. The variational principle given in eqn 1.11 can be generalized to the free boundary case by introducing a surface term to the functional Q

$$Q = \int_0^a \int_0^{2\pi} d\rho d\theta \tilde{L}(R, R_\rho, R_\theta, Z_\rho, Z_\theta, \psi, \psi_\rho) + \eta \int_0^{2\pi} d\theta \tilde{\psi}[\bar{r}(a, \theta)] \left[\frac{\tilde{\psi}[\bar{r}(a, \theta)]}{2} - \psi(a) \right] \quad (3.34)$$

Where L is lagrangian from equation 1.7 and η is constant. Unlike the fixed boundary case, the R and Z variations are now unconstrained. Varying Q

with respect to the dependent variables R and Z yields

$$\begin{aligned} \delta Q = & \int_0^a \int_0^{2\pi} d\rho d\theta \hat{G}(-RZ_\theta \delta R + RR_\theta \delta Z) \\ & + \int_0^{2\pi} d\theta \left(\frac{B^2}{8\pi} (RZ_\theta \delta R - RR_\theta \delta Z) + \eta \left\{ \tilde{\psi}[\tilde{r}(a, \theta)] - \psi(a) \right\} (u_R \delta R + u_Z \delta Z) \right)_{\rho=a} \end{aligned} \quad (3.35)$$

Where $u_R = \delta \tilde{\psi}[\tilde{r}(a, \theta)]/\delta R$ and $u_Z = \delta \tilde{\psi}[\tilde{r}(a, \theta)]/\delta Z$. For simplicity the boundary surface label a was treated as constant in the variations. Note that if $\psi[\tilde{r}(a, \theta)]$ can be expressed explicitly in terms of $\tilde{r}(a, \theta)$, u_R and u_Z are the partial derivatives of $\tilde{\psi}[\tilde{r}(a, \theta)]$ with respect to $R(a, \theta)$ and $Z(a, \theta)$ respectively. Secondly although the term $RZ_\theta \delta R - RR_\theta \delta Z = g^{1/2} \delta \rho(R, Z)$ vanishes at the boundary $\rho = a$ when R and Z are subjected to the fixed boundary constraint, it does not in the free boundary case.

Thus the variational principle derived here may be summarised as follows, In a two-dimensional axisymmetric toroidal system, the equilibrium flux surface geometry described by $\psi(R, Z)$ or parametrically by $R(\rho, \theta)$ and $Z(\rho, \theta)$ is such that the volume integral Q defined in eqn 3.6 is stationary

3.3 Moments equations for the inverse mapping

3.3.1 Determination of fourier expansion coefficients

The variational principle provides well defined algorithm to calculate the fourier amplitudes $R_n(\rho)$ and $Z_n(\rho)$ when n is finite by requiring that Q be stationary with respect to the variations of these amplitudes. Varying Q with respect to a particular amplitude $R_n(\rho)$ or $Z_n(\rho)$ yields the euler equation describing $R_n(\rho)$ or $Z_n(\rho)$

$$\left\langle \frac{\partial \tilde{L}}{\partial R_n} - \frac{\partial}{\partial \rho} \frac{\partial \tilde{L}}{\partial R'_n} \right\rangle = 0 \quad n = 0, 1, \dots \quad (3.36)$$

or

$$\left\langle \frac{\partial \tilde{L}}{\partial Z_n} - \frac{\partial}{\partial \rho} \frac{\partial \tilde{L}}{\partial Z'_n} \right\rangle = 0 \quad n = 1, 2, \dots \quad (3.37)$$

where the prime denotes the differentiation with respect to ρ and $\langle A \rangle$ is the poloidal angle averaging operator defined for any vector A as

$$\langle A \rangle = \int_0^{2\pi} \frac{d\theta}{2\pi} A \quad (3.38)$$

This operator is related to the flux surface averaging operator $\langle A \rangle_f$

$$\langle A \rangle_f = \langle \sqrt{g} A \rangle / \langle \sqrt{g} \rangle \quad (3.39)$$

Although \tilde{L} is defined in 3.12 does not depend on the coordinate Z whereas it does depend on the amplitudes Z_n through Z_θ . These Equations can be shown to be moments of the inverse grad-shafranov equation with basis functions $M_{R_n} = RZ_\theta \cos n\theta$ $M_{Z_n} = RR_\theta \sin n\theta$ or their combination depending on the choice of the poloidal angle θ as in the fixed boundary case discussed above. Moreover the outer boundary conditions can be shown to be moments of equation 3.42 with basis functions $T_{R_n} = u_R \cos n\theta$ $T_{Z_n} = u_Z \sin n\theta$ or their combinations, depending on the choice of θ This explains the appearance of the first term in eqn 3.37

By varying all the amplitudes of fourier series R and Z independently, the euler equations 3.36 3.37 yield

$$\langle M_{R_n} \hat{G} \rangle = 0 \quad n = 0, 1, \dots, n_R \quad (3.40)$$

,

$$\langle M_{Z_n} \hat{G} \rangle = 0 \quad n = 1, 2, \dots, n_Z \quad (3.41)$$

$$\langle T_{R_n} [\tilde{\psi}(\tilde{r}(a, \theta)) - \tilde{\psi}(a)] \rangle = 0 \quad n = 0, 1, \dots, n_R \quad (3.42)$$

and

$$\langle T_{Z_n} [\tilde{\psi}(\tilde{r}(a, \theta)) - \tilde{\psi}(a)] \rangle = 0 \quad n = 1, 2, \dots, n_Z \quad (3.43)$$

The moment equations 3.40 and 3.41 are the same as those in the fixed boundary cases. However equations 3.42 and 3.43 now replace the fixed boundary conditions. Generally the term u_R and u_Z must be evaluated numerically which is computationally expensive. Noting the fact that $\delta\tilde{\psi}[\tilde{r}(a, \theta)]$ is the variation of $\tilde{\psi}[\tilde{r}(a, \theta)]$ at $\tilde{r}(a, \theta)$, a convenient approximation to u_R and u_Z can be obtained by taking $\delta\tilde{\psi}[\tilde{r}(a, \theta)]$ to be the ψ variation at $\tilde{r}(a, \theta)$ then

$$u_R = \psi'(\rho) \frac{RZ_\theta}{g^{1/2}} \quad (3.44)$$

and

$$u_Z = \psi'(\rho) \frac{RR_\theta}{g^{1/2}} \quad (3.45)$$

These provide an accurate approximation to the boundary conditions given in 3.42 and 3.43

where

$$M_{R_n} = RZ_\theta \cos n\theta \quad (3.46)$$

and

$$M_{Z_n} = RR_\theta \sin n\theta \quad (3.47)$$

Alternatively using the convenient Fourier representation

$$R(\rho, \theta) = R_0(\rho) - R_1(\rho) \cos \theta + \sum_{n=2}^{n_R} R_n(\rho) \cos n\theta \quad (3.48)$$

$$Z(\rho, \theta) = E(\rho) \sum_{n=1}^{n_R} R_n(\rho) \sin n\theta \quad (3.49)$$

Where the constraint $Z_n = ER_n$ was imposed the equations for $E(\rho)$ and $R_n(\rho)$ are respectively:

$$\left\langle \left(\sum_{n=1}^{n_R} R_n M_{Z_n} \right) \hat{G} \right\rangle = 0 \quad (3.50)$$

$$\left\langle M_{R_0} \hat{G} \right\rangle = 0 \quad (3.51)$$

$$\left\langle (EM_{Z_1+M_{R_1}}) \hat{G} \right\rangle = 0 \quad (3.52)$$

$$\left\langle (EM_{Z_n} - M_{R_n}) \hat{G} \right\rangle = 0 \quad n = 2, \dots, n_R \quad (3.53)$$

Generally the flux function $F(\psi)$ varies weakly across the plasma cross-section $|F(\rho = a) - F(0)|/|F(0)| \beta_t \ll 1$, where β_t is toroidal beta. The flux surface geometry is therefore sensitive to small inaccuracies in the prescription of the $F(\psi)$ profile. For numerical convenience it has been found useful to eliminate $F(\psi)$ in the moment equations in terms of the total toroidal current enclosed by a flux surfaces $I(\rho) = \int 0^\rho \mathbf{J} \cdot \nabla \phi dV$. Typically $I(\rho)$ vanishes at the magnetic axis $\rho = 0$ and increases monotonically to the value I_0 at the plasma edge, where I_0 is the toroidal plasma current. $I(\rho)$ may be related to the poloidal magnetic field through the surface average of the toroidal component of ampere's law

$$\psi'(\rho) = -\frac{4\pi}{c} \frac{I(\rho)}{\langle g_{\theta\theta} / \sqrt{g} \rangle} \quad (3.54)$$

Furthermore the surface averaged pressure balance equation can be used to eliminate F in terms of I

$$FF'(\psi) = \frac{c}{4\pi} \frac{\langle g_{\theta\theta}/\sqrt{g} \rangle}{\langle \sqrt{g}/g_{\phi\phi} \rangle} I(\rho) \left(\pi c^2 \langle \sqrt{g} \rangle p'(\rho) + \frac{II'(\rho)}{\langle g_{\theta\theta}/\sqrt{g} \rangle} \right) \quad (3.55)$$

Substituting eqns 3.54 and 3.55 into inverse equilibrium operator

$$\begin{aligned} \tilde{G} = & \frac{\mathbf{I}^2(\rho)}{\pi c^2 \sqrt{g} \langle g_{\theta\theta}/\sqrt{g} \rangle} \left(\frac{\partial}{\partial \rho} \frac{g_{\theta\theta}}{\sqrt{g} \langle g_{\theta\theta}/\sqrt{g} \rangle} - \frac{\partial}{\partial \theta} \frac{g_{\rho\theta}}{\sqrt{g} \langle g_{\theta\theta}/\sqrt{g} \rangle} \right) \\ & + \frac{\mathbf{II}(\rho)}{\pi c^2 \langle g_{\theta\theta}/\sqrt{g} \rangle} \left(\frac{g_{\theta\theta}}{g \langle g_{\theta\theta}/\sqrt{g} \rangle} - \frac{1}{g_{\phi\phi}} \right) + p'(\rho) \left(1 - \frac{\langle \sqrt{g} \rangle}{g_{\phi\phi} \langle \sqrt{g}/g_{\phi\phi} \rangle} \right) \end{aligned} \quad (3.56)$$

The green's function $G(\tilde{r}/\tilde{r}')$ is singular when \tilde{r} approaches \tilde{r}' which is related to the self inductance of a toroidal current filament. To remove this singularity when $\theta \rightarrow \theta'$ the self contribution to the poloidal magnetic flux at the boundary surface $\tilde{\psi}[\tilde{r}(a, \theta)]$ is calculated analytically by expanding $G[\tilde{r}(a, \theta)/\tilde{r}'(a, \theta')]$ about θ . $\tilde{\psi}[\tilde{r}(a, \theta)]$ as given by equation 3.24 can be expressed as

$$\begin{aligned} \tilde{\psi}[\tilde{r}(a, \theta)] = & \sum_{m=1}^M G[\tilde{r}(a, \theta)] I_{em} + \frac{I(a)}{\langle \frac{g_{\theta\theta}}{g^{1/2}} \rangle|_a} \left(\int_0^{\theta-\epsilon} + \int_{\theta+\epsilon}^{2\pi} \right) \\ & \frac{d\theta'}{2\pi} \frac{g_{\theta\theta}(a, \theta')}{g^{1/2}} G[\tilde{r}(a, \theta)/\tilde{r}(a, \theta')] + \tilde{\psi}_s \end{aligned} \quad (3.57)$$

Where

$$\tilde{\psi}_s = \frac{4I(a)R(a, \theta)}{c \langle \frac{g_{\theta\theta}}{g^{1/2}} \rangle|_a} \frac{g_{\theta\theta}(a, \theta)}{g^{1/2}} \epsilon \left[\ln \frac{8R(a, \theta)}{\epsilon [g_{\theta\theta}(a, \theta)]^{1/2}} - 1 \right] \quad (3.58)$$

where the moment equations 3.40 3.41 can be written explicitly as

$$\begin{aligned} d_{10}^y r_0''(x) + \sum_{n=2}^{n_R} [d_{1n}^y - E(x)d_{2n}^y] r_n''(x) - \sum_{n=1}^{n_R} r_n d_{2n}^y E''(x) = \\ - \beta_{p0} d_3^y \frac{\hat{p}^2(x)}{\hat{\mathbf{I}}^2(x)} - d_4^y + d_5^y + \sum_{n=1}^{n_R} 2d_{2n}^y E'(x) r_n'(x) \end{aligned} \quad (3.59)$$

where $x = \rho/a$

a is the flux surface label of outermost flux surface list of the variables substituted in 3.59

$$r_n(x) = R_n(\rho)/a \quad (3.60)$$

$$\hat{p}(x) = p(\rho)/p_0 \quad (3.61)$$

$$\hat{I}(x) = I(\rho)/I_0 \quad (3.62)$$

$$\beta_{p_0} = \pi c^2 p_0 a^2 / I_0^2 \quad (3.63)$$

$$d_{1n}^y = \left\langle \left(GS_{1n} - GS_8 \frac{\langle \hat{\tau} GS_{1n} \rangle}{\langle \hat{\tau} GS_8 \rangle} \right) M_y \right\rangle \quad (3.64)$$

$$d_{2n}^y = \left\langle \left(GS_{2n} - GS_8 \frac{\langle \hat{\tau} GS_{2n} \rangle}{\langle \hat{\tau} GS_8 \rangle} \right) M_y \right\rangle \quad (3.65)$$

$$d_y^3 = \langle \hat{\tau} GS_8 \rangle^2 \left\langle \left(GS_3 - GS_4 \frac{\langle \hat{\tau} GS_3 \rangle}{\langle \hat{\tau} GS_4 \rangle} \right) M_y \right\rangle \quad (3.66)$$

$$d_y^4 = \left\langle \left(SS_2 - GS_4 \frac{\langle \hat{\tau} SS_2 \rangle}{\langle \hat{\tau} GS_4 \rangle} \right) \right\rangle \quad (3.67)$$

$$d_y^5 = CS_1 \left\langle \left(GS_8 - GS_4 \frac{\langle \hat{\tau} GS_8 \rangle}{\langle \hat{\tau} GS_4 \rangle} \right) M_y \right\rangle \quad (3.68)$$

where M_y are basis functions i.e M_E and M_{R_n}

$$GS_{1n} = \frac{z_{\theta\theta} \hat{g}_{\theta\theta}}{r \hat{\tau}^3} \cos n\theta \quad (3.69)$$

$$GS_{2n} = \frac{r_{\theta\theta} \hat{g}_{\theta\theta}}{r \hat{\tau}^3} \sin n\theta \quad (3.70)$$

$$GS_3 = r \quad (3.71)$$

$$GS_4 = 1/r \quad (3.72)$$

$$GS_5 = z_\theta / r^2 \hat{\tau} \quad (3.73)$$

$$GS_6 = \frac{1}{r \hat{\tau}^3} [\hat{g}_{\theta\theta} (r_x z_{x\theta} - r_{x\theta} z_x) + \hat{g}_{\rho\theta} (r_{\theta\theta} z_x + r_\theta z_{x\theta} - r_{x\theta} z_\theta - r_x z_{\theta\theta})] \quad (3.74)$$

$$GS_7 = \frac{1}{r \hat{\tau}^2} (r_\theta r_{x\theta} + z_\theta z_{x\theta} - r_x r_{\theta\theta} - z_x z_{\theta\theta}) \quad (3.75)$$

$$GS_8 = \hat{g}_{\theta\theta} / r \hat{\tau}^2 \quad (3.76)$$

$$CS_1 = \frac{1}{\langle \hat{\tau} GS_8 \rangle} \left\langle \frac{\hat{g}_{\theta\theta x}}{\sqrt{\hat{g}}} - \frac{\hat{g}_{\theta\theta} r_x}{r_2 \hat{\tau}} + \frac{(r_x z_{x\theta} - r_{x\theta} z_x) \hat{g}_{\theta\theta}}{r \hat{\tau}^2} \right\rangle \quad (3.77)$$

$$SS_2 = GS_5 + GS_6 + GS_7 + GS_8 \frac{\hat{I}'(x)}{\hat{I}(x)} \quad (3.78)$$

where $\hat{\tau}, \sqrt{\hat{g}}, g_{\mu\nu}, r$ and z are the corresponding normalized quantities.

Given the plasma pressure and toroidal current $p(\rho)$ and $I(\rho)$ respectively eqn 3.59 defines a set of coupled second order ODE's for the Fourier amplitude functions $R_n(\rho)$ and $E(\rho)$ which is calculated to solve the set of moment equations with the boundary conditions varying with respect to external circuit using a shooting technique.

3.4 Derived quantities

3.4.1 Volume

The differential volume is given by

$$dV = \sqrt{g} dp d\theta d\phi \quad (3.79)$$

Integrating out the variables lead to

$$\frac{dV}{d\rho} = 4\pi^2 \langle \sqrt{g} \rangle \quad (3.80)$$

3.4.2 Flux tube surface area

The surface area enclosing a flux tube generated by rotating a given flux contour completely around 2π radians in the ϕ direction is given by

$$S = 4\pi^2 \langle \sqrt{g} |\nabla\rho| \rangle \quad (3.81)$$

3.4.3 Poloidal flux

The surface average of the toroidal component of Ampere's law gives

$$\chi^{(\rho)} = -\frac{(4\pi/c)I(\rho)}{\langle g_{\theta\theta}/\sqrt{g} \rangle} \quad (3.82)$$

where χ is defined by

$$|\nabla\chi(\rho)| = 2\pi R B_p \quad (3.83)$$

3.4.4 Poloidal current

Similarly, the poloidal current enclosed between the axis of symmetry and the magnetic surface ρ

$$F(\rho) = \frac{c}{2} R B_T(R) \quad (3.84)$$

can be written in terms of the moments by surface averaging the pressure balance equation

$$\langle \sqrt{g} \tilde{G} \rangle = 0 \quad (3.85)$$

to give

$$F^2(\rho) = F_0^2 \left\{ 1 + \frac{1}{q_0^2 A^4} \int_{\rho}^a \frac{d\rho}{\langle \sqrt{g}/g_{\phi\phi} \rangle} \left[\frac{2\beta_{p_0} \langle \sqrt{g} \rangle}{p_0 a^2} + \frac{I'^2}{I_0^2 \langle g_{\theta\theta}/\sqrt{g} \rangle} \right] \right\} \quad (3.86)$$

where

$$F_0 = \frac{c}{2} R_G B_T(R_G) \quad (3.87)$$

$$q_0 = F_0/I_0 A^2 \quad (3.88)$$

and

$$A = R_G/a \quad (3.89)$$

3.4.5 Toroidal flux

$$\Phi(\rho) = \frac{4\pi}{c} \int_0^\rho F(\rho) \left\langle \frac{\sqrt{g}}{g_{\theta\theta}} \right\rangle d\rho \quad (3.90)$$

3.4.6 Toroidal current density

$$j_\phi(\rho, \theta) = -j_{\phi 0} \frac{\langle g_{\theta\theta}/\sqrt{g} \rangle I_0}{I(\rho)} \left[\frac{\beta_{T_0} a p'(\rho) [R(\rho, \theta)/R_G]^2}{p_0} + \frac{a F F'(\rho)}{F_0^2} \right] \frac{R_G}{R(\rho, \theta)} \quad (3.91)$$

where

$$j_{\phi 0} = F_0^2/2\pi a R_G I_0 \quad (3.92)$$

and

$$\beta_{T_0} = \pi p_0 R_G^2 c^2 / F_G^2 \quad (3.93)$$

3.4.7 Equivalent Current density

$$\tilde{j}(\rho) = \langle \sqrt{g} j_\phi(\rho, \theta) / R \rangle / \langle \sqrt{g} / R \rangle \quad (3.94)$$

where

$$I(\rho) = \int_0^\rho \tilde{j}(\rho) dA \quad (3.95)$$

with

$$dA = 2\pi \langle \tau \rangle d\rho \quad (3.96)$$

3.4.8 Safety factor

$$q(\rho) = \frac{d\Phi}{d\chi} = q_0 A^2 \frac{\hat{F}}{\hat{I}} \left\langle \frac{\sqrt{g}}{g_{\phi\phi}} \right\rangle \left\langle \frac{g_{\theta\theta}}{\sqrt{g}} \right\rangle \quad (3.97)$$

3.5 Numerical Formulation

The set of moment eqn 3.59 is a coupled system of second order ODEs for the unknown $r_0(x), r_n(x)$ $n \geq 2$ and $E(x)$. A solution requires two boundary conditions for each moment equation. The so called 'Fixed boundary condition' provides one of these per equation by specifying the shape of the outermost flux surface

$$r_n(a) = r_{na} \quad (n = 0, 2, \dots) \quad (3.98)$$

$$E(a) = E_a \quad (3.99)$$

The remaining boundary conditions are obtained by requiring that the poloidal magnetic flux $\chi(R, Z)$ be analytic at magnetic axis. i.e. that the flux contours be concentric ellipses near the magnetic axis. They are given by

$$r_0(0) = r_m \quad (3.100)$$

$$E(0) = E_m \quad (3.101)$$

$$r_n(0) = 0 \quad (n = 2, \dots) \quad (3.102)$$

and

$$r_0' = 0 \quad (3.103)$$

$$E'(0) = 0 \quad (3.104)$$

$$r_n'(0) = 0 \quad (n = 2, \dots) \quad (3.105)$$

The conditions (3.100)-(3.105) define $\rho = 0$ as a critical point of the system and special numerical steps must be taken to avoid this singularity. The solution space in ρ is contracted from $[0, a]$ to $[\delta_0 a, a]$ where δ_0 is a small positive number. The analytic properties of the solutions of r_n, E near the origin $\rho = 0$ are then used to rewrite eqns 3.100-3.105 as

$$r_0(\delta_0) = r_m - \lambda_1 \delta_0^2 \quad (3.106)$$

$$r_n(\delta_0) = r_{n_0} (\delta_0^n)^2 \quad (n = 2, \dots) \quad (3.107)$$

and

$$E(\delta_0) = E_m + \lambda_2 \delta_0^2 \quad (3.108)$$

Where λ_1 and λ_2 are arbitrary small positive constants. The solutions obtained are insensitive to exact values of λ_1 and λ_2 .

The corresponding boundary conditions on the derivatives are then

$$r_0'(\delta_0) = 2\lambda_1 \delta_0 \quad (3.109)$$

$$r'_n(\delta_0) = 2nr_{n_0}\delta_0^{2n-1} \quad (n = 2, \dots) \quad (3.110)$$

$$E'(\delta_0) = 2\lambda_2\delta_0 \quad (3.111)$$

The set of amplitude functions r_n and E_n is infinite. To model an equilibrium plasma at finite beta, It is useful to consider only a finite number of amplitude functions r_n . Our experience and that of others indicate that the set r_0, r_2, E with $n_R = 2$ is sufficient for most cases. The resulting finite set of equations can be written as

$$Ay'' = b \quad (3.112)$$

Where the elements of matrix \mathbf{A}

$$A = \begin{pmatrix} a_{11} & a_{12} & a_{13} \\ a_{21} & a_{22} & a_{23} \\ a_{31} & a_{32} & a_{33} \end{pmatrix} \quad (3.113)$$

are functions of the unknown vector y

$$y = [r_0(x), E(x), r_2(x)] \quad (3.114)$$

and its first derivatives. The vector b is a function of y, y' and the driving functions $p'(x), I(x)$ and $I'(x)$

To solve the system of equations (3.112), ‘the well known shooting method’ is employed using NAG’s subroutine D02AGF . The system is rewritten as a set of six first order ODE’s with solution vectors defined now as explicit functions of a parameter vector \hat{p}

$$\tilde{\mathbf{y}} = (y_1, y'_1, y_2, y'_2, y_3, y'_3) = \tilde{y}(x; \tilde{\mathbf{p}}) \quad (3.115)$$

$$\tilde{\mathbf{A}}\tilde{\mathbf{y}}' = \tilde{\mathbf{b}} \quad (3.116)$$

with the components of \hat{p} defined in terms of the six remaining unknown boundary conditions. A solution of the ODE system is obtained by solving a parameter estimation problem for \hat{p} .

The numerical method used to solve the set of moment equations through 3.59 is similar to that used in fixed boundary case which is discussed in detail in Ref 1 and Ref 2. The moment equation through 1alp through 2alp are rewritten as a set of first order differential equations. The fixed boundary at $\rho = a$ are now replaced by the free boundary conditions given in eqns 3alp through 4alp and the equations relating the boundary surface label a to the limiter coordinates. The system of equation is then posed as a parameter estimation problem and is solved using a shooting technique. The differential equations are integrated using runge-kutta merson method and iterated using a modified Newton’s method

Chapter 4

Results

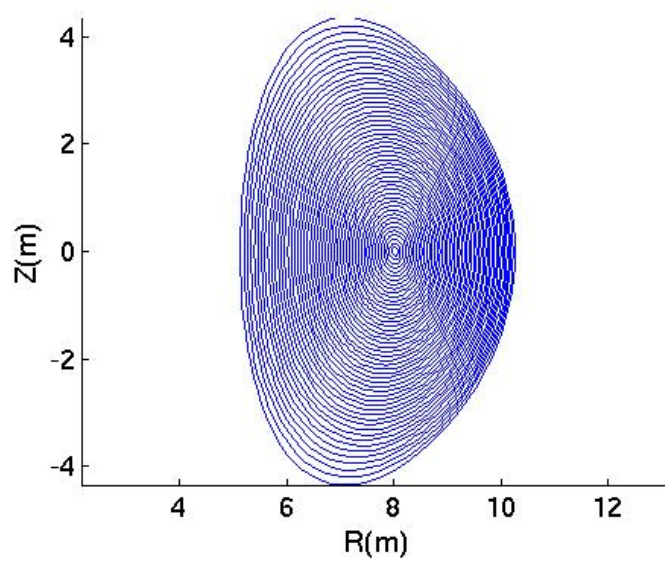
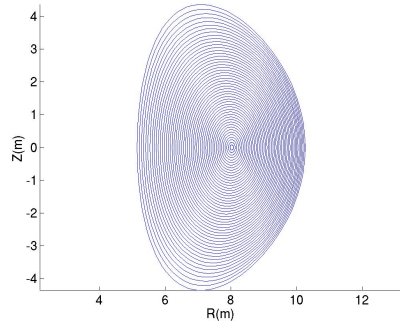
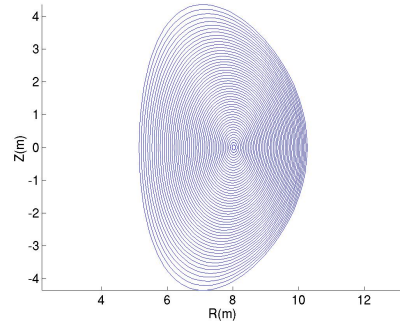


Figure 4.1: Flux surface contour in Cylindrical coordinate system

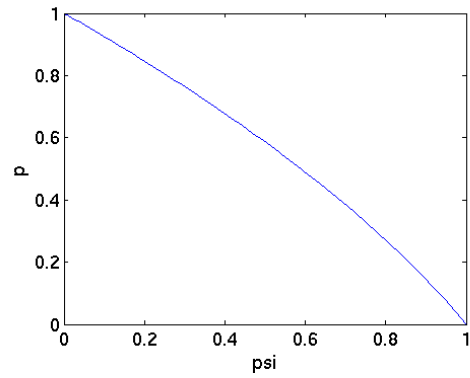
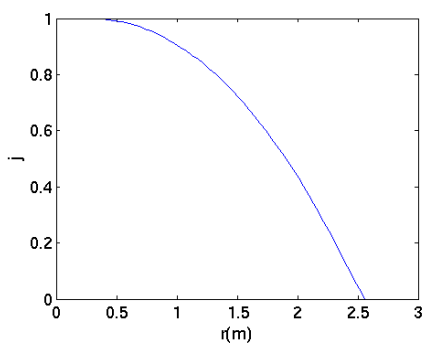
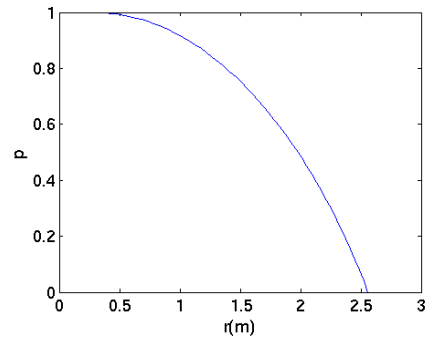
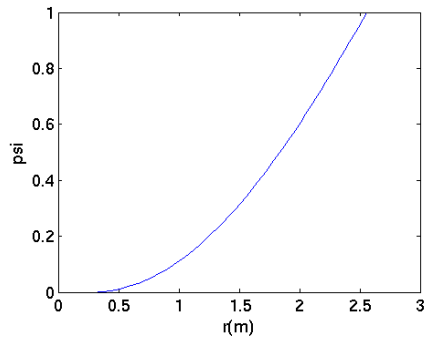
All computational work is done fortran 77 and plotting is done in python.

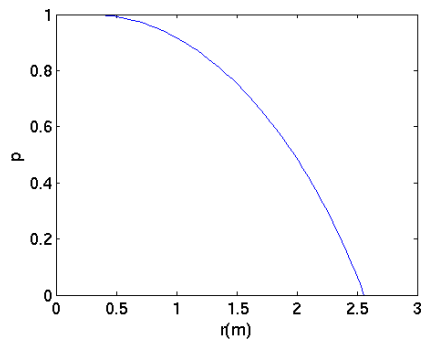
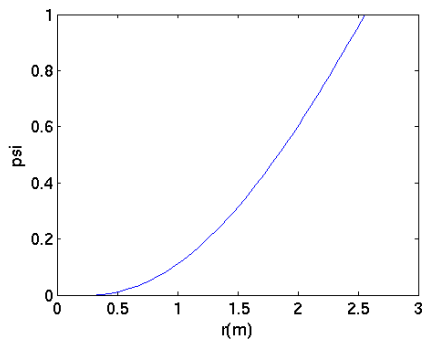
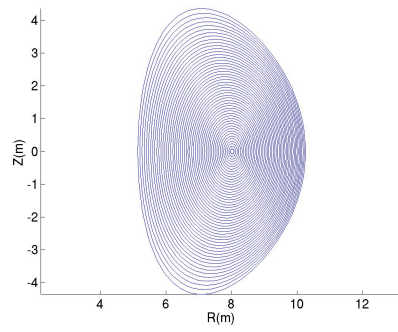
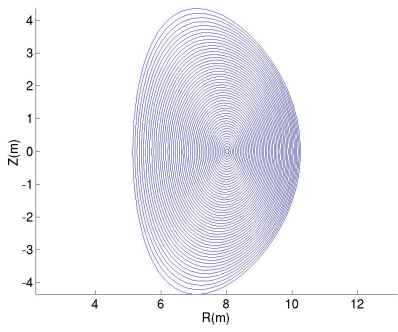
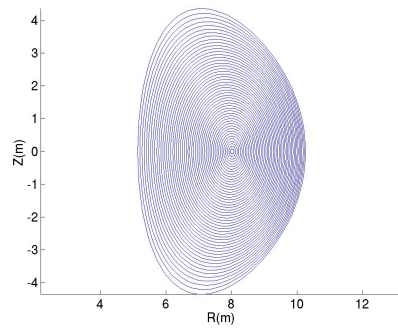
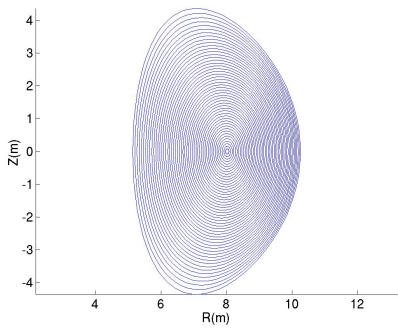
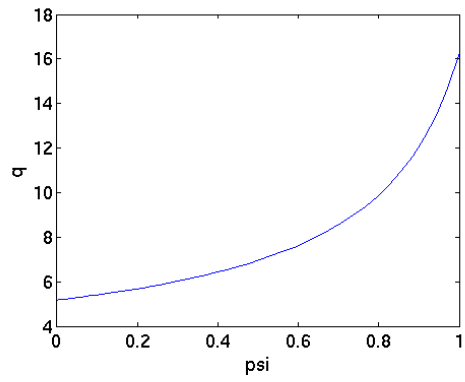


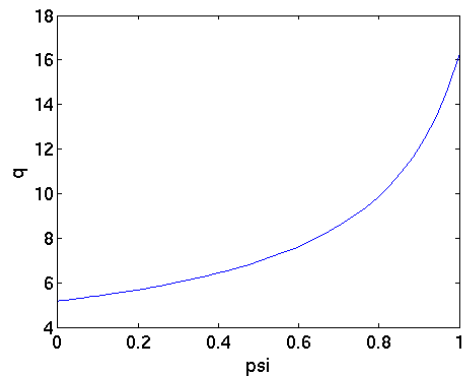
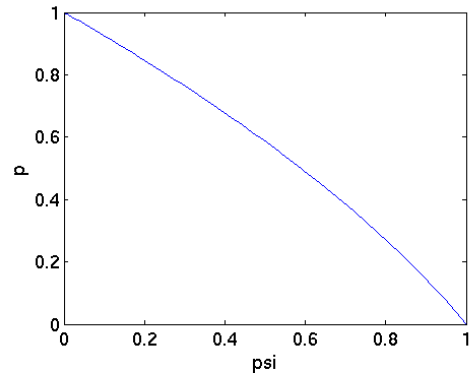
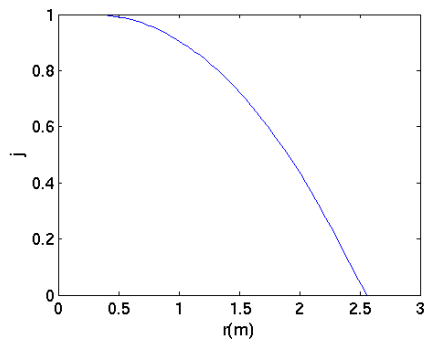
(a) caption 1



(b) caption 2







Chapter 5

Discussion

This code is patched yet to calculate the flux surfaces while including the external circuits in the system which will be further extended to calculate the flux and other plasma parameter a X point (separatrix) and strike points that is the location of plasma particle when it hits the divertor plate. It will be included in 2-D vmoms code and extended to arbitrary order of moments simultaneously too. The amount of computational time required for the moment method depends on the number of amplitudes functions being determined and on the relative error desired so that Fourier amplitudes are calculated upto order of two . The moment method is faster by a factor of 10 or more in computational speed while reproducing the same equilibrium with a degree of accuracy sufficient for many purposes.

References

- [1] V. D. Shafranov, Sov. Phys. JETP 6, 545 (1958).
- [2] V. D. Shafranov, Zh. Eksp. Teor. Fiz. 33, 710 (1957).
- [3] L.L. Lao, S.P. Hirshman and R.M. Wieland, Phys. Fluids 24 (1981) 1431.
- [4] L.L. Lao, R.M. Wieland, W.A. Houlberg and S.P. Hirshman, Comput. Phys. Comm. 27, 129 (1982)
- [5] Numerical Algorithms Group (NAG) Library Manual, Downer's Grove, IL, Mark 8 (1981).
- [6] J.L. Johnson et. al , J. Comput. Phys. 32, 212 (1979)
- [7] A. Portone, Nucl. Fusion 44, 265 (2004)
- [8] R. Srinivasan, S. Chaturvedi, S.P. Deshpande Fusion. Engine. and Design 70, 269 (2004)
- [9] R. Srinivasan, L.L. Lao, M.S. Chu, Plasma Phys. Control. Fusion, 52, (2010), 035007
- [10] J. P. Freidberg, Rev. Mod. Phys. 54, 801 (1982).
- [11] L.D. Landau, E.M. Lifshitz, Fluid Mechanics, Second Edition, Volume 6
- [12] L.S. Solov'ev, JETP, 6,26 (1968)